Research Paper
J. Astron. Space Sci. 33(1), 45-54 (2016)
http://dx.doi.org/10.5140/JASS.2016.33.1.45

JASS Journal of Astronomy and Space Sciences

Improved GPS-based Satellite Relative Navigation Using Femtosecond Laser Relative Distance Measurements

Hyungjik Oh[1], Han-Earl Park[2], Kwangwon Lee[1], Sang-Young Park[1†], Chandeok Park[1]
[1]Astrodynamics and Control Lab., Department of Astronomy, Yonsei University, Seoul 03722, Korea
[2]Korea Astronomy and Space Science Institute, Daejeon 34055, Korea

This study developed an approach for improving Carrier-phase Differential Global Positioning System (CDGPS) based real-time satellite relative navigation by applying laser baseline measurement data. The robustness against the space operational environment was considered, and a Synthetic Wavelength Interferometer (SWI) algorithm based on a femtosecond laser measurement model was developed. The phase differences between two laser wavelengths were combined to measure precise distance. Generated laser data were used to improve estimation accuracy for the float ambiguity of CDGPS data. Relative navigation simulations in real-time were performed using the extended Kalman filter algorithm. The GPS and laser-combined relative navigation accuracy was compared with GPS-only relative navigation solutions to determine the impact of laser data on relative navigation. In numerical simulations, the success rate of integer ambiguity resolution increased when laser data was added to GPS data. The relative navigational errors also improved five-fold and two-fold, relative to the GPS-only error, for 250 m and 5 km initial relative distances, respectively. The methodology developed in this study is suitable for application to future satellite formation-flying missions.

Keywords: relative navigation, global positioning system, carrier-phase measurements, femtosecond laser, integer ambiguity resolution

1. INTRODUCTION

The Global Positioning System (GPS) is a well-used satellite navigation technology (Parkinson et al. 1996; Hofmann-Wellenhof et al. 2001). Numerous space missions have applied GPS systems to meet navigational accuracy requirements. For example, the PRISMA mission, which is a mission for the Earth observation using hyperspectral sensors, applied GPS-based relative navigation to perform autonomous formation flying (D'Amico et al. 2013). When performing GPS-based relative navigation, the Carrier-phase Differential GPS (CDGPS) concept is widely used and several formation-flying missions have used CDGPS to obtain relative navigation solutions. For example, during the Gravity Recovery and Climate Experiment (GRACE) mission, the CDGPS-based relative navigation error was ~2 cm in the radial and cross-track directions, and 4 cm in the along-track direction, in comparison with K-band inter-satellite ranging measurements (Kroes et al. 2005; Montenbruck et al. 2005; Kohlhase et al. 2006). The TerraSAR-X and TanDEM-X missions also used CDGPS-based relative navigation to attain millimeter-level resolution of the Synthetic Aperture Radar (SAR) interferometric baseline (Montenbruck et al. 2008).

The single/double differencing method has advantages to the GPS-based relative navigation. GPS satellites' clock errors, receivers' clock errors, and ionospheric errors can also be eliminated by differencing two individual GPS raw data measurements obtained from two GPS receivers (Hofmann-Wellenhof et al. 2001). Relative navigation accuracy using carrier measurements is typically at millimeter-level, while code measurement-based relative navigation accuracy is about three orders of magnitude

Received Oct 2, 2015 **Revised** Jan 26, 2016 **Accepted** Jan 27, 2016
†**Corresponding Author**
E-mail: spark624@yonsei.ac.kr, ORCID: 0000-0002-1962-4038
Tel: +82-2-2123-5687, Fax: +82-2-392-7680

higher. In pseudorange measurements, clock errors between GPS satellites and the receiver significantly increase distance measurement errors. For CDGPS, the error factor mainly reflects GPS integer ambiguity resolution (i.e., the number of carrier waves that have traveled from GPS satellites to the receiver). When GPS integer ambiguity is exactly known, millimeter-level carrier-phase measurement precision can be achieved (Hofmann-Wellenhof et al. 2001). Park et al. (2010) obtained centimeter-level three dimensional (3D) Root-Mean-Square (RMS) position accuracy in hardware-in-the-loop simulations of formation-flying satellites using millimeter-level carrier-phase measurement data.

Many space missions have applied the Least-squares AMBiguity Decorrelation Adjustment (LAMBDA) method (Teunissen 1995) to resolve double difference carrier-phase ambiguity. The LAMBDA method applies a general least-squares approach to estimate the integer ambiguity contained in carrier-phase measurements. In the float ambiguity resolution phase, precise inter-satellite baseline information increases the ambiguity resolution rate and resolution accuracy (Hofmann-Wellenhof et al. 2001). Precise float ambiguity solutions can improve the accuracy of integer ambiguity resolution and can reduce resolution time. Thus, more accurate integer ambiguity resolutions can yield better relative navigational results.

The main objective of this study was to establish a method of utilizing laser data to improve the accuracy of integer ambiguity resolutions. Satellites' relative distance measurement data was applied to a GPS measurement model to improve the quality of the ambiguity resolution. A femtosecond laser using a synthetic wavelength interferometry (SWI) algorithm was used to measure the distance between two satellites. Since the configuration of femtosecond lasers is simple and all parts are composed of optical fiber, they can be operated reliably with external vibration and shock, such that they can fit within the extreme environment of space. A software-in-the-loop simulation was performed to describe the laser measurement data, which were applied to the CDGPS-based relative navigation algorithm. An Extended Kalman Filter (EKF) algorithm was applied to obtain a real-time relative navigation solution. The results showed that success rates of integer ambiguity resolution increased when the laser data were included.

2. RELATIVE NAVIGATION ALGORITHM

2.1 Dynamic Model

In GPS technology (Fig. 1), target satellites A and B are both equipped with GPS receivers that obtain GPS measurement data. The states of target satellites A and B are represented by:

$$\vec{\mathrm{X}}_{AB}(t) = [\vec{r}_A(t), \vec{v}_A(t, \vec{r}_A), \vec{r}_{AB}(t), \vec{v}_{AB}(t, \vec{r}_A, \vec{r}_B)]^{\mathrm{T}} \quad (1)$$

where $\vec{r}_A(t)$ and $\vec{v}_A(t, \vec{r}_A)$ are the position and velocity vector of satellite A, respectively, and relative position and velocity between satellite A and B are represented by $\vec{r}_{AB}(t)$ and $\vec{v}_{AB}(t, \vec{r}_A, \vec{r}_B)$, respectively. The state vectors are propagated and estimated by this filtering algorithm. The relative state vector of the satellite B with respect to the satellite A

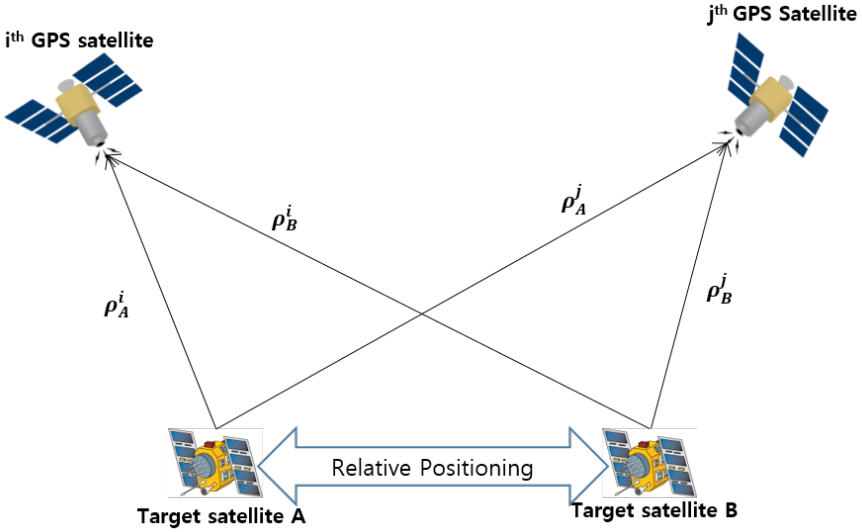

Fig. 1. Concept of satellite relative positioning using the Global Positioning System (GPS).

is presented in relative frame (RSW coordinate system). The R axis is from the geocentric radius vector, the W axis is normal to the position vector and the velocity vector of the satellite A, and the S axis is perpendicular to the R axis and the W axis. The equation of motion for a satellite is expressed using the two-body equation with perturbations (Vallado 2013), which is expressed as:

$$\ddot{\vec{r}} = -\frac{\mu}{r^3}\vec{r} + \vec{a}_{perturbed} \tag{2}$$

In this study, perturbing acceleration ($\vec{a}_{perturbed}$) contained the effects of the non-spherical gravity of the Earth, solar radiation pressure, solar and lunar gravity, and atmospheric drag.

2.2 GPS Measurement Model

GPS measurements conceptually indicate the signal travel time from GPS satellites to a GPS receiver. Time differences between the transmission time from the GPS satellites and receiving time of the receiver are measured with Coarse/Acquisition (C/A) code or carrier-phase measurements, and are typically referred to as pseudorange data (Hofmann-Wellenhof et al. 2001). The C/A code pseudorange at specific time (t) can be modeled by:

$$R_A^i(t) = \rho_A^i(t) + c\Delta\delta_A^i(t) \tag{3}$$

where $R_A^i(t)$ is the code pseudorange measured between satellite A and the i^{th} GPS satellite, and $\rho_A^i(t)$ is the geometrical distance between the receiver and the GPS satellite. Clock bias $\Delta\delta_A^i(t)$ is multiplied to the speed of light (c) to represent clock error. When two receivers' code pseudorange measurements are differenced, the linearized single difference code pseudorange $\Delta y_{P,AB}^i$ is obtained by:

$$\Delta y_{P,AB}^i = (\Delta\hat{\boldsymbol{e}}_{AB^*}^i)^T\delta\vec{r}_A + (\Delta\hat{\boldsymbol{e}}_{B^*}^i)^T\delta\vec{r}_{AB} + c\delta t_{AB} \tag{4}$$

where $\hat{\boldsymbol{e}}_{AB}^i$ is a unit vector calculated by differencing the pseudorange data of receivers A and B of the i^{th} GPS satellite and superscript * is estimated position of the satellite. The mathematical model of the carrier-phase measurement pseudorange is expressed as:

$$\Phi_A^i(t) = \frac{1}{\lambda}\rho_A^i(t) + N_A^i + f^i\Delta\delta_A^i(t) \tag{5}$$

where $\Phi_A^i(t)$ is the carrier-phase, λ indicates the wavelength and clock bias $\Delta\delta_A^i(t)$ for the carrier-phase measurement multiplied to the GPS satellites' signal frequency f^i, and N_A^i is the integer ambiguity of the wavelength.

When measurement data of the i^{th} and j^{th} GPS satellites are successfully acquired by receivers A and B, the following single difference equations can be derived:

$$\Phi_{AB}^i(t) = \frac{1}{\lambda}\rho_{AB}^i(t) + N_{AB}^i + f^i\Delta\delta_{AB}^i(t) \tag{6}$$

$$\Phi_{AB}^j(t) = \frac{1}{\lambda}\rho_{AB}^j(t) + N_{AB}^j + f^j\Delta\delta_{AB}^j(t) \tag{7}$$

When the i^{th} and j^{th} GPS satellite measurement data have the same frequency, the time biases of the receivers can be eliminated. Linearized CDGPS measurements are derived by differencing equations (6) and (7) through the expression:

$$\nabla\Delta y_{\Phi,AB}^{ij} = (\nabla\Delta\hat{\boldsymbol{e}}_{AB^*}^{ij})^T\delta\vec{r}_A + (\nabla\hat{\boldsymbol{e}}_{B^*}^{ij})^T\delta\vec{r}_{AB} + \lambda\nabla\Delta N_{AB}^{ij} \tag{8}$$

2.3 Laser Measurement Model

In this study, a laser distance measurement model was integrated with the GPS single/double difference measurement model. Jang et al. (2014) introduced the use of a femtosecond laser based on an SWI algorithm to make relative distance measurements of formation-flying satellites. The optical comb of a femtosecond laser is mode-locked so that the frequency is very stable (Kim et al. 2005). Harmonic wavelength can be generated by using several wavelengths that correspond to multiples of the mode space, and is applied to construct interferometry of the synthetic wavelength to measure distance.

The precision of laser measurement data is affected by relative distance (ρ_{AB}) and relative velocity ($\dot{\rho}_{AB}$). The relative velocity between spacecraft mainly affects measurement precision owing to measuring latency that occurs from the low-pass-filter in the SWI algorithm. To describe this phenomenon, a Scale Factor (SF; κ) of relative velocity was applied to the laser measurement model. We set SF to $-5.15E^{-3}$, based on the work of Jung et al. (2012), who investigated empirical femtosecond laser measurement data simulations. The laser measurement model (L_{AB}) was considered to be a function of ρ_{AB} and $\dot{\rho}_{AB}$ (Jung et al. 2012), and is expressed as:

$$L_{AB} = \rho_{AB} + \kappa\dot{\rho}_{AB} + \omega_L \tag{9}$$

where ω_L is the laser measurement noise. When this model is linearized by relative position and relative velocity, Eq. (10) is derived:

In this study, the linearized GPS code, carrier-phase measurement model, and laser measurement model were combined (e.g., Eqs. 4, 8 and 10) to form Eq. (11):

$$y_{L,AB} = (\hat{\boldsymbol{r}}_{AB^*})^T \delta \boldsymbol{r}_{AB} + \kappa \frac{1}{\rho_{AB^*}} \{(\dot{\boldsymbol{r}}_{AB^*})^T - \dot{\rho}_{AB^*} (\hat{\boldsymbol{r}}_{AB^*})^T\} \delta \boldsymbol{r}_{AB} + \kappa (\hat{\boldsymbol{r}}_{AB^*})^T \delta \dot{\boldsymbol{r}}_{AB} \tag{10}$$

$$\begin{bmatrix} \Delta y^{j}_{P,AB} \\ \nabla \Delta y^{ij}_{\Phi,AB} \\ y_{L,AB} \end{bmatrix} = \begin{bmatrix} (\Delta \hat{\boldsymbol{e}}^{i}_{AB^*})^T & \emptyset_{n\times 3} & (\Delta \hat{\boldsymbol{e}}^{i}_{B^*})^T & \emptyset_{n\times 3} & c_{n\times 1} & \emptyset_{n\times 3} \\ (\nabla \Delta \hat{\boldsymbol{e}}^{ij}_{AB^*})^T & \emptyset_{(n-1)\times 3} & (\nabla \hat{\boldsymbol{e}}^{ij}_{B^*})^T & \emptyset_{(n-1)\times 3} & \emptyset_{(n-1)\times 1} & \lambda_{(n-1)\times(n-1)} \\ \emptyset_{1\times 3} & \emptyset_{1\times 3} & (\hat{\boldsymbol{r}}_{AB^*})^T + \kappa \frac{1}{\rho_{AB^*}} \{(\dot{\boldsymbol{r}}_{AB^*})^T - \dot{\rho}_{AB^*} (\hat{\boldsymbol{r}}_{AB^*})^T\} & \kappa (\hat{\boldsymbol{r}}_{AB^*})^T & \emptyset_{1\times 1} & \emptyset_{1\times(n-1)} \end{bmatrix} \begin{bmatrix} \delta \boldsymbol{r}_A \\ \delta \dot{\boldsymbol{r}}_A \\ \delta \boldsymbol{r}_{AB} \\ \delta \dot{\boldsymbol{r}}_{AB} \\ \delta t_{AB} \\ \nabla \Delta N^{ij}_{AB} \end{bmatrix} \tag{11}$$

where subscript n denotes the number of observable GPS satellites.

The ambiguity of GPS carrier-phase measurements was also determined. When GPS measurement data are solely utilized, the upper two columns in Eq. (11) are only applied to the measurement model in the filtering algorithm. The ambiguity of the GPS carrier-phase can be estimated using GPS measurements only. However, when the laser measurement data and model are added to the algorithm, the unknown parameters in Eq. (11), including the ambiguity, can be estimated more accurately, in particular when laser measurement data accuracy is high.

2.4 Filtering Algorithm

In this study, the estimating filter of Kalman (1960) was utilized for real-time satellite navigation. The EKF uses a state transition matrix in a linearized form to predict covariance (Zarchan & Musoff 2005). The relative navigation algorithm was performed based on the relative state vector, initial estimation of the covariance matrix, the process noise (Q), and the measurement noise (R). The relative state vector of the satellite B with respect to the satellite A was represented in RSW coordinates. The predicted covariance matrix (P) and state in the EKF process are expressed as:

$$P_k^- = \Phi P_{k-1} \Phi^T + Q \tag{12}$$

$$X_k^- = f(X_{k-1}) \tag{13}$$

where superscript – is the propagated state and subscript k indicates the step number of the filtering process. The Kalman gain is calculated using the predicted covariance (P_k^-), and both the GPS and laser-combined measurement model (H), as expressed in equation (14):

$$K_k = P_k^- H_k^T \left(H_k P_k^- H_k^T + R\right)^{-1} \tag{14}$$

Compared with the relative navigation algorithm performed using GPS data only, the laser distance measurements and model can improve the estimation precision of the Kalman gain, updated state, and covariance. When the CDGPS model is added to the EKF algorithm, the states to be determined contain carrier-phase float ambiguity. When the float ambiguity is resolved to high precision, the error of integer ambiguity resolution also can be reduced. Satellite states and the covariance is updated using:

$$X_k^+ = X_k^- + K_k (z - H_k X_k^-) \tag{15}$$

$$P_k^+ = P_k^- - K_K H_k P_k^- \tag{16}$$

In equations (15) and (16), the state vector of the satellite A in Earth-Centered Inertial (ECI) coordinates is obtained from GPS-based absolute navigation, while the relative state vector can be induced by coordinate transformation. Relative navigation is subsequently performed by applying laser relative distance measurements. The state vector of the satellite B can be calculated by adding the relative state vector to that of the satellite A. Both satellite states are propagated until the next filtering step.

2.5 Ambiguity Resolution

Integer ambiguities must be determined in order to make significant use of carrier-phase measurement data. If integer ambiguity has been resolved correctly, the measurement error using carrier-phase measurements will be less than 19 cm, which reflects the length of the GPS L1 signal. After float ambiguity resolution is completed by the filtering algorithm, the integer ambiguity has to be determined. The most common integer ambiguity resolution method is LAMBDA (Teunissen 1995), which was developed to solve the problem that correlation in the off-diagonal term of the covariance matrix increases integer ambiguity resolution processing time. Rapid integer ambiguity resolution is possible with non-correlated re-defined float ambiguity and a covariance matrix. True integer ambiguity is resolved by reverse conversion of the estimated integer ambiguity.

Table 1. Initial positions and velocities of satellite A and B

	Radius of the projected circular orbit			
	250 m × 500 m		5 km × 10 km	
Satellite	A	B	A	B
X (m)	6,930,000	6,930,250	6,930,000	6,935,000
Y (m)	0	0	0	0
Z (m)	0	0	0	0
V_x (m/s)	0	0	0	0
V_y (m/s)	3,810.947	3,810.815	3,810.947	3,808.307
V_z (m/s)	6,600.754	6,600.525	6,600.754	6,596.182

3. RELATIVE NAVIGATION SIMULATION

3.1 Simulation Settings

Relative navigational simulations using GPS and laser measurement data were performed for two formation-flying satellites. The initial relative distance between the satellites was set to 250 m and 5 km, and both were Projected onto a Circular Orbit (PCO) by considering the availability of formation-flying satellites in Low Earth Orbit (LEO). The initial position and velocity components of two satellites in the ECI coordinate system are presented in Table 1. Total simulation time was set to 100 min, with GPS and laser measurement data obtained every second. GPS signals were simulated using the GSS6560 Spirent Global Navigation Satellite System (GNSS) signal simulator and Spirent SimGEN program, while the AsteRx space-borne GPS receiver was used to obtain raw GPS measurements (Park et al. 2010). The number of observable GPS satellites is presented in Fig. 2. Laser measurement data were generated using software algorithms, including possible Gaussian random error introduced by hardware characteristics. When more than four GPS satellites were observable, relative navigation was available, which occurred for the whole simulation time.

Simulation was started by propagating the true states from the initial state of the satellite A and B. For the dynamic propagation of satellite states, the Earth's gravity, the gravity of the sun and the moon, the air drag, and solar radiation were considered. GPS and laser measurements were generated by corresponding algorithms and the simulator. The generated data were transmitted to the satellite on-board computer module to perform the extended Kalman filter based relative navigation.

3.2 Simulation Results

Figs. 3 and 4 show the laser measurement data, measurement rates, and measurement errors. Measurement errors were calculated by subtracting the generated laser data from the true relative position of two spacecraft. The characteristics of the femtosecond laser causes proportional relation between distance rate and distance error. Due to the latency existing in low-pass filter of the femtosecond laser algorithm, distance-measuring delay is occurred. Therefore, the error between true

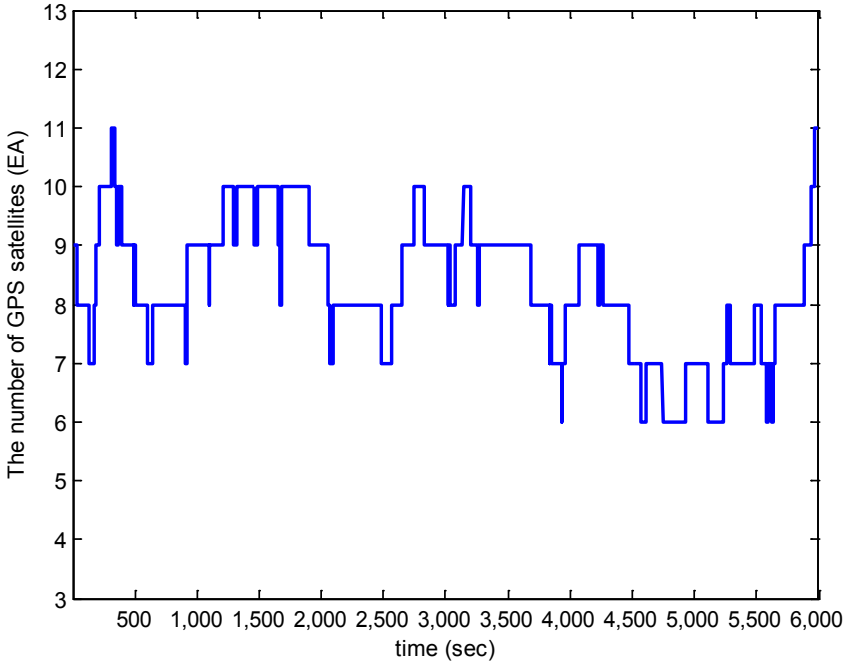

Fig. 2. Number of observable Global Positioning System (GPS) satellites with total simulation period.

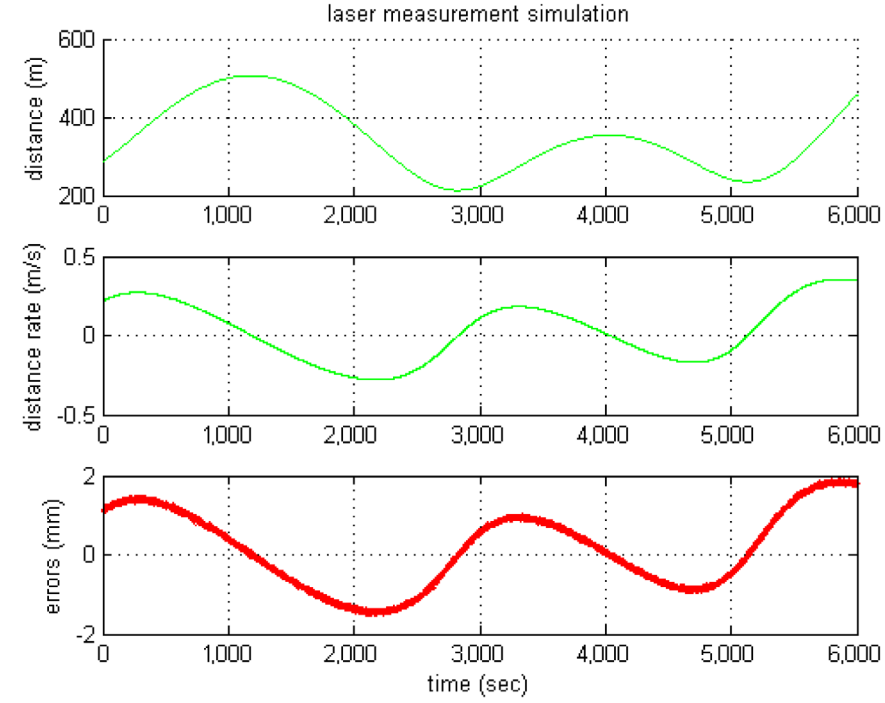

Fig. 3. Laser data simulation results for a 250 m initial relative distance.

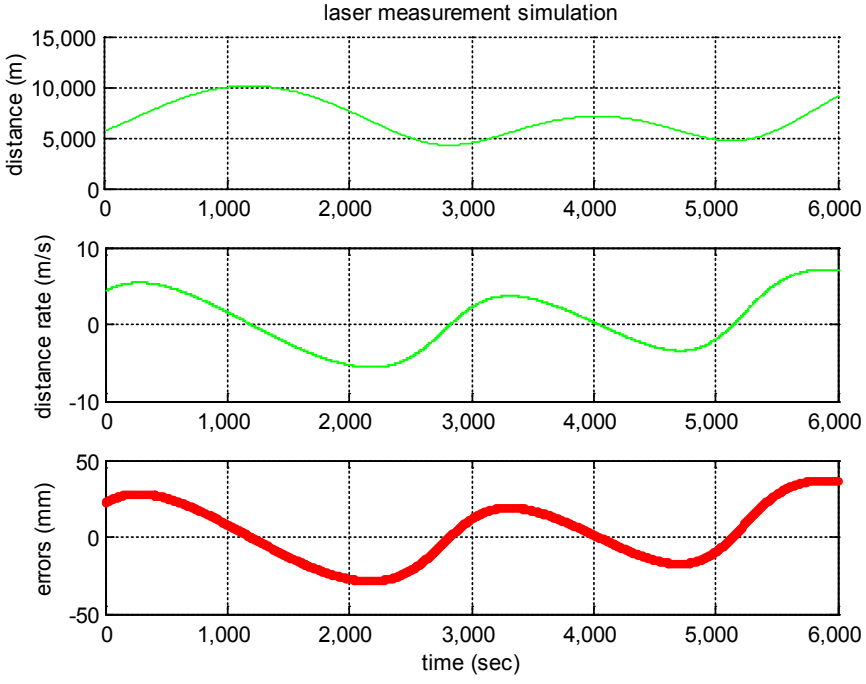

Fig. 4. Laser data simulation results for a 5 km initial relative distance.

relative distance and the laser measurements become larger when the rate of the relative distance change is higher. Figs. 5 and 6 show GPS-based relative navigational errors for the 250 m initial relative distance. The errors were calculated from the difference between simulated true states and estimated states and are expressed in terms of RMS. When integer ambiguity was not estimated, relative navigational error increased to decimeter level (Figs. 5 and 6). Relative navigational errors for when laser data were added to the simulation are presented in Figs. 7 and 8. In these simulations, integer ambiguities were fully estimated for all simulation times. The results showed that 3D relative navigational RMS errors decreased from 10.68 mm

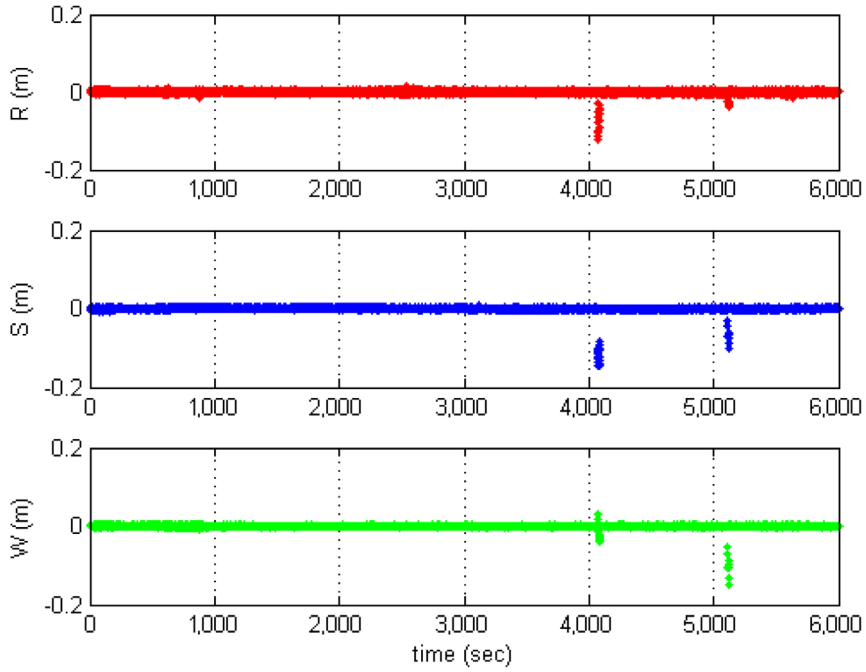

Fig. 5. Relative navigational errors using Global Positioning System (GPS) data in RSW coordinates for a 250 m initial relative distance.

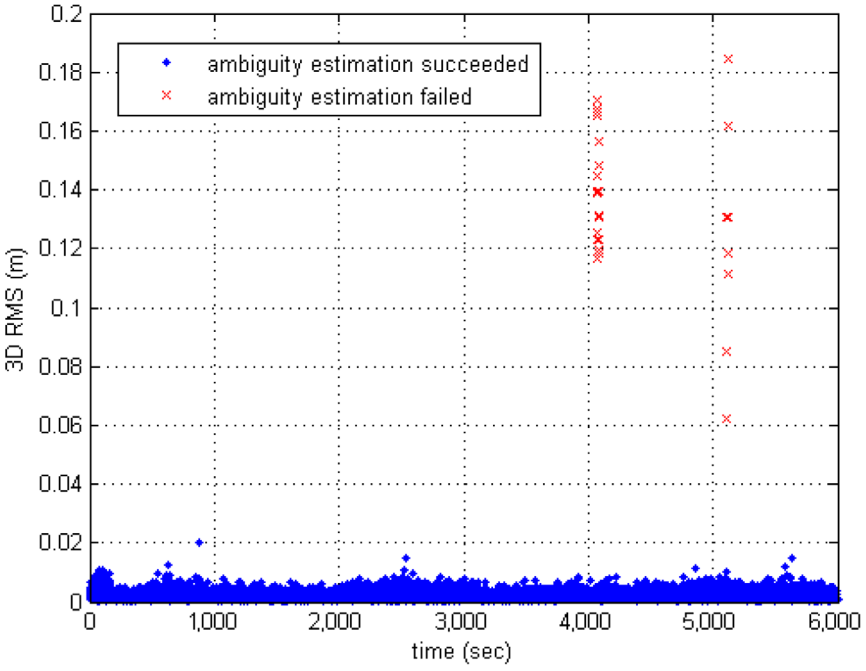

Fig. 6. Relative navigational errors using Global Positioning System (GPS) data in 3-dimensional space for a 250 m initial relative distance. Dots indicate successfully estimated integer ambiguity, and crosses show failed integer ambiguity resolution.

to 2.11 mm, reflecting the increase in the integer ambiguity resolution success rate for the CDGPS data. Rates of integer ambiguity resolution success according to the total simulation time are increased from 99.55% to 100% when laser data were applied.

The results of simulations performed using the 5 km initial relative distance are shown in Figs. 9 and 10, and Table 2. Relative navigational errors increased as the relative distance between the satellites was extended. When only GPS measurements were applied, the 3D RMS error was

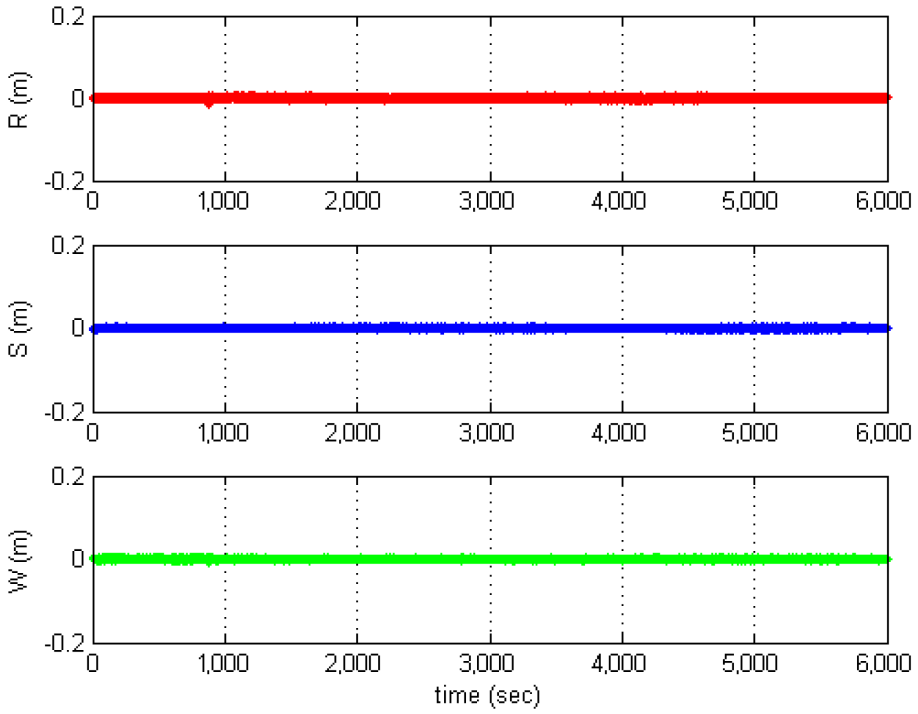

Fig. 7. Relative navigation errors using Global Positioning System (GPS) data and laser data in RSW coordinates for a 250 m initial relative distance.

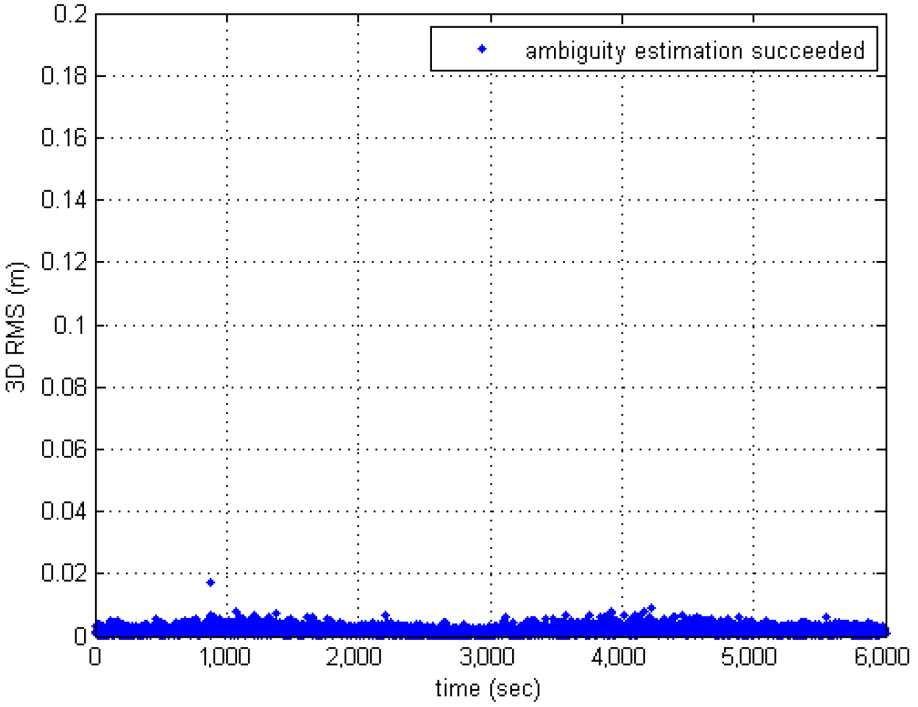

Fig. 8. Relative navigational errors using Global Positioning System (GPS) data and laser data in 3-dimensional space for a 250 m initial relative distance.

29.78 mm, but this decreased to 14.05 mm when laser measurement data were added. The integer ambiguity resolution success rate also increased significantly. These simulation results imply that the application of laser relative distance measurement data to GPS-based relative navigation is more effective for longer relative distances.

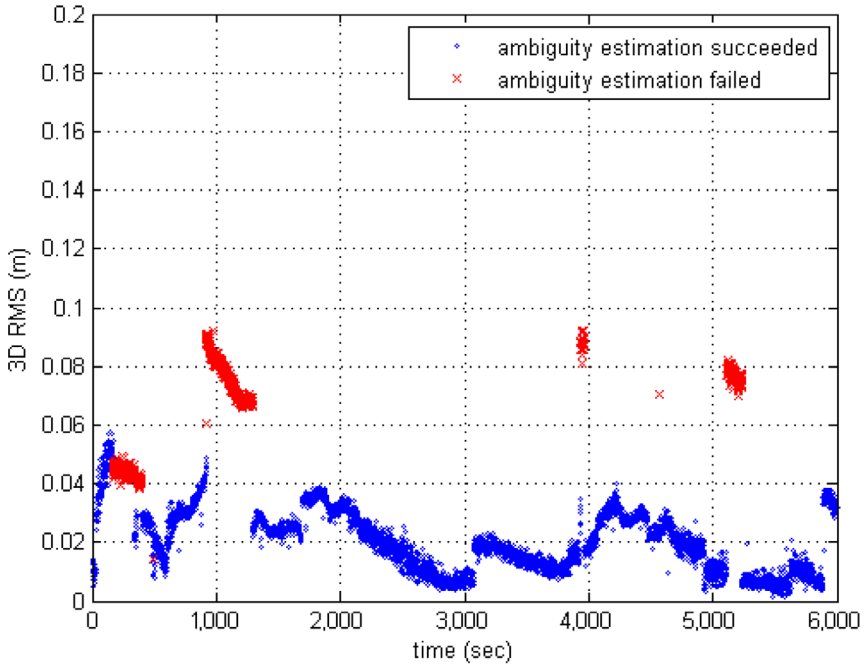

Fig. 9. Relative navigational errors using Global Positioning System (GPS) data in 3-dimensional space for a 5 km initial relative distance. Blue data points indicate successful estimations, and red data show failed estimations.

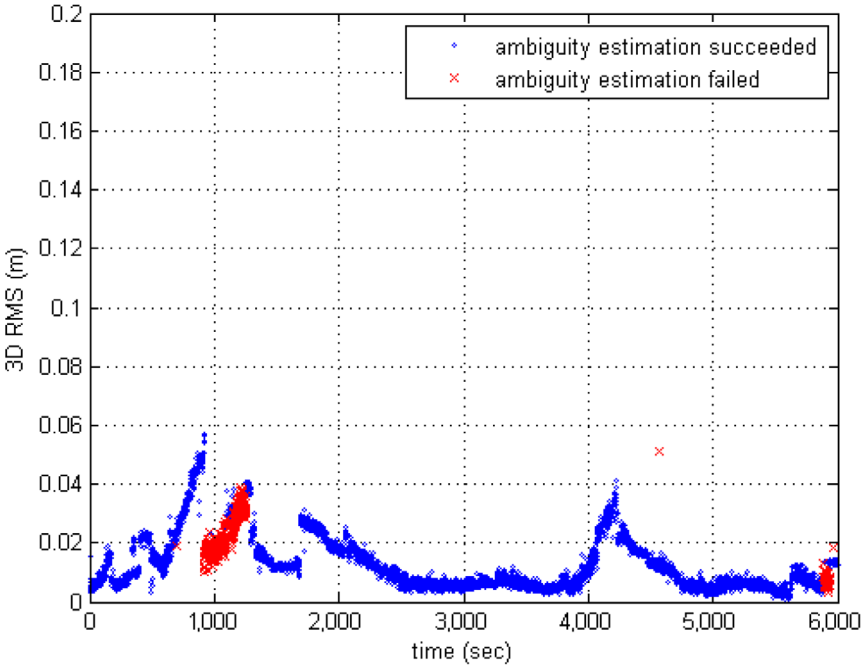

Fig. 10. Relative navigational errors using Global Positioning System (GPS) data and laser data in 3-dimensional space for a 5 km initial relative distance. Blue data points indicate successful estimations, and red data show failed estimations.

Table 2. Relative navigational error with and without laser distance measurement data

Radius of the projected circular orbit	Measurement data type	R (mm)	S (mm)	W (mm)	3D RMS (mm)	Integer ambiguity resolution rate (%)
250 m × 500 m	GPS only	5.11	7.92	5.00	10.68	99.55
	GPS + laser	1.55	1.05	0.95	2.11	100
5 km × 10 km	GPS only	12.70	24.32	10.73	29.78	87.39
	GPS + laser	10.13	8.68	3.87	14.05	94.2

4. CONCLUSIONS

In this study, we proposed a new approach to improving GPS-based satellite relative navigation using femtosecond laser-based relative distance measurements. Synthetic wavelength interferometry-based femtosecond laser, which was chosen for its high robustness to space environments, was applied to CDGPS-based relative navigation to improve the performance of float ambiguity resolution. When performing the software simulation using 250 m and 5 km initial relative distances on PCO, the integer ambiguity resolution success rate increased when laser data was added. The resulting relative navigation solutions showed five-fold and two-fold improvements for the 250 m and 5 km initial relative distances, respectively. The increases in the integer ambiguity resolution success rate were caused by the positive effects of the laser-based baseline measurement data on CDGPS-based relative navigation. During the EKF process, a laser measurement model was added to the single/double difference GPS measurement model, resulting in higher precision estimation accuracy. In conclusion, the femtosecond laser represents a useful tool for future formation-flying missions that require high precision relative navigational requirements. Furthermore, femtosecond laser-based baseline measurement data can be utilized to verify relative baseline determination results.

ACKNOWLEDGMENTS

This work was supported by Global Surveillance Research Center (GSRC) program funded by the Defense Acquisition Program Administration (DAPA) and Agency for Defense Development (ADD) of Korea.

REFERENCES

D'Amico S, Ardaens JS, Florio SD, Autonomous formation flying based on GPS-PRISMA flight results, Acta Astron. 82, 69-79 (2013). http://dx.doi.org/10.1016/j.actaastro.2012.04.033

Hofmann-Wellenhof B, Lichtenegger H, Collins J, GPS Theory and Practice (Springer, New York, 2001).

Jang YS, Lee K, Han S, Lee J, Kim YJ, et al., Absolute distance measurement with extension of nonambiguity range using the frequency comb of a femtosecond laser, Opt. Eng. 53, 122403 (2014). http://dx.doi.org/10.1117/1.OE.53.12.122403

Jung S, Park SY, Park HE, Park C, Kim SW, et al., Real-Time Determination of Relative Position Between Satellites Using Laser Ranging, J. Astron. Space Sci. 29, 351-362 (2012). http://dx.doi.org/10.5140/JASS.2012.29.4.351

Kalman RE, A New Approach to Linear Filtering and Prediction Problems, J. Basic Eng. 82, 35-45 (1960). http://dx.doi.org/10.1115/1.3662552

Kim YS, Jin JH, Joo KN, Kim SW, Absolute distance measurement using synthetic wavelength of femto-second laser, Proceedings of the Korean Society for Precision Engineering, JeJu, Korea, 23-24 June 2005.

Kohlhase AO, Kroes R, D'Amico S, Interferometric Baseline Performance Estimations for Multistatic Synthetic Aperture Radar Configurations Derived from GRACE GPS observations, J. Geodesy 80, 28-39 (2006). http://dx.doi.org/10.1007/s00190-006-0027-y

Kroes R, Montenbruck O, Bertiger W, Visser P, Precise GRACE baseline determination using GPS, GPS Solut. 9, 21-31 (2005). http://dx.doi.org/10.1007/s10291-004-0123-5

Montenbruck O, Van Helleputte T, Kroes R, Gill E, Reduced dynamic orbit determination using GPS code and carrier measurements, Aerosp. Sci. Technol. 9, 261-271 (2005). http://dx.doi.org/10.1016/j.ast.2005.01.003

Montenbruck O, Kahle R, D'Amico S, Ardaens J, Navigation and control of the TanDEM-X formation, J. Astronaut. Sci. 56, 341-357 (2008). http://dx.doi.org/10.1007/BF03256557

Park JI, Park HE, Park SY, Choi KH, Hardware-in-the-loop simulations of GPS-based navigation and control for satellite formation flying, Adv. Space Res. 46, 1451-1465 (2010). http://dx.doi.org/10.1016/j.asr.2010.08.012

Parkinson BW, Spilker Jr JJ, Axelrad P, Enge P, Global Positioning System: Theory and Applications (American Institute of Aeronautics and Astronautics, Virginia, 1996).

Teunissen PJG, The least-squares ambiguity decorrelation adjustment: a method for fast GPS integer ambiguity estimation, J. Geodesy 70, 65-82 (1995). http://dx.doi.org/10.1007/BF00863419

Vallado DA, Fundamentals of Astrodynamics and Applications (Microcosm Press, California, 2013).

Zarchan P, Musoff H, Fundamentals of Kalman filtering: a practical approach, (American Institute of Aeronautics and Astronautics, Virginia, 2005).